

***Ab initio* studies of structural and electronic properties of the crystalline $\text{Ge}_2\text{Sb}_2\text{Te}_5$**

Geunsik Lee and Seung-Hoon Jhi*

Department of Physics, Pohang University of Science and Technology, Pohang 790-784, Republic of Korea

(Received 22 October 2007; revised manuscript received 2 March 2008; published 2 April 2008)

We study the atomic structure and the electronic and optical properties of $\text{Ge}_2\text{Sb}_2\text{Te}_5$ in two different crystalline states of cubic and hexagonal structures with the use of *ab initio* pseudopotential density functional method. It is found that electronic and atomic structures are very sensitive to the layer sequence in the two phases. The proximity of vacancy layer to Ge layer leads to the splitting of Ge-Te bond length, which, in turn, affects the electronic and optical properties. The effect of Te *d* orbitals is also investigated with respect to structural properties.

DOI: [10.1103/PhysRevB.77.153201](https://doi.org/10.1103/PhysRevB.77.153201)

PACS number(s): 61.50.Ah, 64.70.K-, 71.15.Mb

Phase-change random access memory (PRAM) is one of the most promising candidates for the next generation non-volatile memories. The 225 phase ($\text{Ge}_2\text{Sb}_2\text{Te}_5$ or GST in short) is the simplest and most promising and has thus been extensively studied. The GST is known to undergo a series of structural transitions at elevated temperature from nonconducting amorphous (*a*) to metastable cubic (*c*) and to a more stable hexagonal above 300 °C. Pulse current-driven melting (above ~ 600 °C) and quenching switch the crystalline phase to high-resistive amorphous phase. The rapid and reversible cycles between the amorphous and crystalline structures lead to the resistivity change that reads as the on-off state of PRAM (Ref. 1 and references therein). Recently, the $a \leftrightarrow c$ transition has actively been investigated by extended x-ray absorption fine structure (EXAFS).¹⁻³ The flip of Ge atoms from octahedral to tetrahedral sites was proposed as a mechanism for the rapid $a \leftrightarrow c$ transition,² but detailed atomic structures in the process are still yet to be known. The metastable cubic phase has a rocksalt structure, in which cations (Ge, Sb) and vacancies randomly occupy the fcc sublattice and Te wholly occupies the other sublattice.⁴ An intermediate state during the transformation to the stable hexagonal phase was also observed with a rearrangement of cations to form ordered layers.⁵ For the hexagonal phase, there have been controversies about the layer sequence along the [0001] direction. Kooi and De Hosson proposed a layer sequence of Te-Ge-Te-Sb-Te-Te-Sb-Te-Ge-.⁶ Petrov *et al.* proposed a layer sequence with interchanged Ge and Sb layers.⁷ On the other hand, Matsunaga *et al.* suggested a model in which Ge and Sb atoms are randomly distributed in each cation layer.⁸ Recently, first principles calculations⁹ showed that the layer sequence proposed by Kooi and De Hosson is more stable than the model in Ref. 7.

As for the electrical properties, the Hall measurement^{10,11} showed *p*-type conduction with a carrier concentration of about $10^{20}/\text{cm}^3$ for both cubic and hexagonal phases. The temperature dependence of the conductivity, on the other hand, indicated that the hexagonal phase exhibits a metallic characteristic, while the cubic phase behaves like a semiconductor. This observation seems inconsistent with the measured optical gap of 0.5 eV for both phases.^{10,12} The vacancies are considered to play an important role in the electrical conduction,^{12,13} but the conduction mechanism is not yet clearly understood. One possible origin of the different electrical properties is the ordered (disordered) arrangement of

vacancies in hexagonal (cubic) phase and the layer sequence. In this Brief Report, we report the atomic structures and electronic and optical properties of GST with the use of *ab initio* pseudopotential density functional method. Of particular interest is the structure and layer-sequence dependence of these properties.

For the total energy calculations, the Vienna *ab initio* simulation package (VASP)¹⁴ is used. The exchange correlation of electrons is treated within the generalized gradient approximation (GGA) in the form of Perdew-Wang 1991.¹⁵ The projected augmented wave pseudopotentials are used as provided in the package.¹⁶ The cutoff energy for plane-wave basis expansion is chosen to be 13 Ry. The atomic structures are relaxed until the error in total energy is less than 1 meV/atom. It is well known that the semicore *d* orbitals cannot be ignored for correct descriptions of the atomic and electronic structures of many III-V and II-VI semiconductors.^{17,18} Here, we carry out calculations both with and without Te 4*d* orbitals as valence to investigate how the Te *d* orbitals affect bonding characteristics in GST. Since Te pseudopotential with 4*d* as valence is not provided in the package, we instead generate Te pseudopotential with 4*d* orbitals by following a norm-conserving pseudopotential scheme and calculate the atomic structures of the hexagonal phase for comparison. The cutoff energy is chosen to be 30 or 70 Ry for the calculations in the norm-conserving pseudopotential plane-wave basis method without or with Te *d* orbitals, respectively.

Total energies of GST are calculated for two crystalline phases: the hexagonal closed pack (hcp) and face-centered-cubic (fcc) structures. For the crystalline phases, we consider the two different layer sequences of Kooi and De Hosson⁶ (Te-Ge-Te-Sb-Te-Te-Sb-Te-Ge-) and Petrov *et al.*⁷ (Te-Sb-Te-Ge-Te-Te-Ge-Te-Sb-) along the [0001] direction of hcp (or the [111] direction of fcc) as depicted in Fig. 1. Our calculated results of the energies and lattice parameters are summarized in Table I. The inclusion of Te *d* orbital significantly affects the structural properties, such as interatomic distance, which was also frequently observed for III-V and II-VI compounds.^{17,18} Compared to the experiment, calculations with Te *d* orbitals included as valence seem more accurate and appropriate. However, qualitative features are preserved whether or not Te 4*d* is included. This will also be true for the fcc structure as it has an almost identical local atomic structure to hcp for a given layer sequence (Te *d* orbital is not included as valence for the fcc structure). For

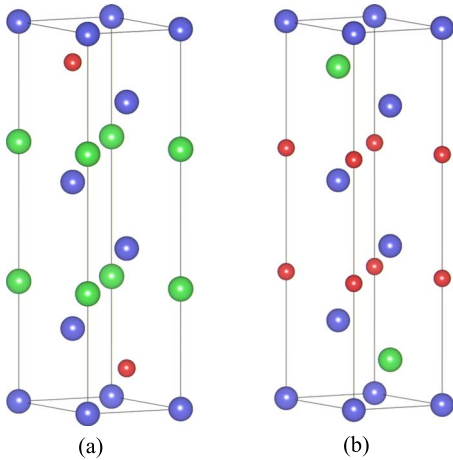


FIG. 1. (Color online) The schematic layer sequences in hexagonal phase $\text{Ge}_2\text{Sb}_2\text{Te}_5$ for sequences of (a) Kooi and De Hosson (Ref. 6) and (b) Petrov *et al.* (Ref. 7). The red (small, dark gray), green (large, light gray), and blue (large, dark gray) balls denote Ge, Sb, and Te atoms, respectively. The same layer sequences are also used for cubic phase along its (111) direction.

the structural stability, our calculation shows that the Kooi–De Hosson⁶ sequence has a slightly larger cohesive energy than the sequence of Petrov *et al.*⁷ for both crystalline phases, which is consistent with previous calculations and supports the observation by Kooi and De Hosson.⁶ Measured structural parameters show a large variation depending on sample preparation and measurement techniques. Particularly, the c -axis lattice constant and the layer sequence are quite scattered. A transmission electron microscopy measurement reported the c -axis lattice constants of 18.27 and 16.96 Å for the sequences of Kooi and De Hosson and Petrov *et al.*, respectively,^{6,7} while x-ray diffraction on powder samples showed a mixed sequence of Kooi and De Hosson⁶ and Petrov *et al.*⁷ with a c -axis lattice constant of 17.24 Å.⁸ When Te d orbitals are included as valence, our calculated c -axis lattice constant is close to that reported in Ref. 7. However, the difference in the c axis lattice constants for the two sequences is not consistent between this calculation and

the measurement. Calculated cohesive energies and lattice constants alone are unable to exclusively pinpoint the layer sequences compared to experiment. We study the structure and layer-sequence dependence of local atomic structures and electronic and optical properties to further address a plausible sequence, as discussed below. Measurements on the cubic phase, on the other hand, reported almost the same lattice constant of about 6.02 Å. With six layers per each cube along the $[111]$ direction considered, this value corresponds to the hexagonal (c -axis) lattice constant of 17.38 Å, including nine atomic and one additional vacancy layers. Our calculated value is larger than the experimental one, which can be partly attributed to the ordering effect of cations and vacancies in our model. With cations and vacancies randomly distributed in a given layer (with a bigger supercell), our calculations showed that the lattice constant of the fcc structure tends to decrease as the distribution becomes more random (a slight increase in unit cell volume of about $\sim 5\%$ is observed). It is possible that repeated cycles of annealing and heating make the structure have the ordered cation layer, as assumed in this study, which was actually observed in experiment.⁵

One important characteristic in our results is the cation-anion bond length. The sequence of Petrov *et al.*⁷ has two different bond lengths for Ge-Te, whereas the Kooi–De Hosson⁶ sequence has almost a single Ge-Te bond length. This is compared to the Sb-Te bond, which does not show such sequence dependence. The splitting in Ge-Te bond indicates that Ge layers in the sequence of Petrov *et al.*⁷ lie closer to one of the two neighboring Te layers. This observation was not affected by the choice of Te d orbitals as valence. The proximity of vacancy layer to Ge layer in the sequence of Petrov *et al.*⁷ leads to the splitting, which is interpreted as a stronger interaction between Ge-vacancy layers than between Sb-vacancy layers. The splitting is also consistent with the fact that GST is one of the several phases found in the solid solutions of GeTe and Sb_2Te_3 , where only Ge atoms proximate to vacancy are more likely to be decomposed into two constituents. The repeated calculations in a double-sized unit cell with the sequences of Kooi and De Hosson⁶ and Petrov *et al.*⁷ coexisting came to the same con-

TABLE I. Calculated relative cohesive energies ΔE_c (meV/atom), lattice constants (Å), and interatomic distances (Å) of the two crystal structures: hcp (H) and fcc (C) phases of $\text{Ge}_2\text{Sb}_2\text{Te}_5$ with two different layer sequences [Kooi and De Hosson (Ref. 6) and Petrov *et al.* (Ref. 7)]. For the fcc structure, the lattice parameters are converted to those of equivalent hcp axes. The Kooi–De Hosson (Ref. 6) sequence is more stable than the sequence of Petrov *et al.* (Ref. 7) for both hcp and fcc, according to our results. Calculations with the Te d orbitals are also carried out for the hexagonal phase (marked by *).

| Sequence | Phase | ΔE_c | a | c | Ge-Te | Sb-Te | Te-Te |
|-----------------------------------|-------|--------------|------|-------|------------|------------|-------|
| Kooi and De Hosson ^a | H* | 34 | 4.17 | 16.87 | 2.94, 2.95 | 2.93, 3.07 | 3.78 |
| Petrov <i>et al.</i> ^b | H* | 0 | 4.15 | 17.07 | 2.78, 3.13 | 2.95, 3.08 | 3.75 |
| Kooi and De Hosson ^a | H | 10 | 4.01 | 16.41 | 2.85, 2.86 | 2.89, 2.97 | 3.40 |
| Petrov <i>et al.</i> ^b | H | 0 | 4.07 | 16.28 | 2.75, 3.00 | 2.90, 3.00 | 3.47 |
| Koo and De Hosson ^a | C | 17 | 4.29 | 17.70 | 3.00, 3.02 | 3.01, 3.20 | 4.16 |
| Petrov <i>et al.</i> ^b | C | 0 | 4.25 | 18.24 | 2.84, 3.29 | 3.02, 3.19 | 4.20 |

^aReference 6.

^bReference 7.

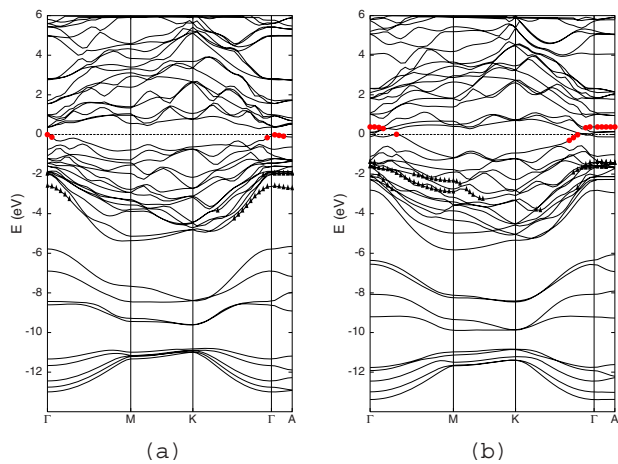


FIG. 2. (Color online) Calculated band structures of the hexagonal $\text{Ge}_2\text{Sb}_2\text{Te}_5$ with the layer sequences of (a) Kooi and De Hosson (Ref. 6) and (b) Petrov *et al.* (Ref. 7). The states denoted by red (dark gray) circles are mostly associated with Te lone-pair states, whereas the states denoted by black triangles have a significant contribution from the bonding with neighboring cations.

clusion, indicating that the short-range layer sequence is more important for the cation-anion bonding than the long-range ordering. The study of Ge-Te bond length can thus give some insights into the bonding characteristics associated with the transition related to local layer sequencing.

The splitting of Ge-Te bond length was actually found in experiment.^{2,8,19} For the cubic phase, the atomic pair distribution showed a broad distribution for Ge-Te bonding with two distinct peaks at 2.81 and 3.25 Å, which are compared to that of 2.92 and 3.12 Å for Sb-Te.¹⁹ The EXAFS study of the cubic phase showed a similar difference in bond lengths of 2.83 and 3.2 Å for Ge-Te and 2.91 and 3.2 Å for Sb-Te with somewhat large error bars.² Measured interatomic distances in the hexagonal phase showed a similar splitting for Ge-Te (2.90 and 3.20 Å) and Sb-Te (2.99 and 3.05 Å).⁸ The Te-Te bond length was measured to be about 3.75 Å, which is quite close to our calculation of the sequence of Petrov *et al.*⁷ However, the diffraction data were claimed to be best fit with the model of a mixed sequence of Kooi and De Hosson⁶ and Petrov *et al.*^{7,8} Overall, our calculated bond lengths imply that experimental results can be better explained if we assume the sequence of Petrov *et al.*⁷

To investigate the effect of layer sequence on electrical properties, we calculate the band structure of the GST. Figure 2 shows the calculated band structures of the hexagonal phase in the two layer sequences. Here, the Te *d* orbitals are treated as cores as the band structures are less sensitive to Te *d* orbital. Once the *d* orbitals are included, the top of valence bands shifts upward due to *p-d* coupling,¹⁸ which slightly reduces the band gap, if it exists. Our calculation showed that the cubic phase has almost the same band structure as the hexagonal phase for a given layer sequence (not shown here). This implies that the contrasting electrical properties of cubic and hexagonal phases^{10,11} can be attributed to a different tendency of layer sequences in the two structures. One caveat is that in this study, as the vacancies are assumed to be ordered for both crystalline phases, not

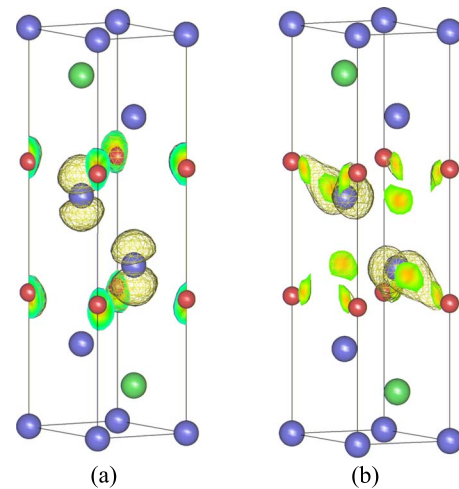


FIG. 3. (Color online) Isocharge surfaces of (a) a red (filled-circle) and (b) a black-triangle state shown in Fig. 2(b) (Petrov sequence). Ge, Sb, and Te atoms are represented by the red (small, dark gray), green (large, light gray), and blue (large, dark gray) balls, respectively.

only the layer sequence but also the disordering in vacancy distribution can significantly affect the electronic structures. The upper valence bands mainly have *p*-orbital characters and the low-lying valence bands are derived from *s* orbitals of both cation and anion. Similar to structural properties, the band structure also exhibits a strong sequence dependence. The energy gap of Kooi and De Hosson⁶ was calculated to be about 0.26 eV, whereas the sequence of Petrov *et al.*⁷ was found not to have a gap. It is rather unusual that the Jahn-Teller-type distortion in Ge-Te bond length in the sequence of Petrov *et al.*⁷ leads to the closure of band gap, which is, in fact, found to be related to the lone-pair states derived from Te layers.

As the states associated with vacancy layers are important for conduction, we identify the states derived from tellurium lone pairs (LPs) by projecting wave functions onto each atom in the unit cell. The tellurium LPs are caused by vacancies near Te atoms. There are two tellurium atoms that have such LPs in the hexagonal unit cell. We assign a state as an LP state if the projection to *p* orbitals of the two tellurium atoms near the vacancy layer is larger than half the total projection. These states are indicated in Fig. 2 as red (dark gray) circles. For comparison, Te-derived states, which have a significant bonding with neighboring cations, are denoted by filled triangles. The isocharge surface in Fig. 3 explicitly shows the bonding characteristics of the LP and Te-derived states. As shown in Fig. 2, the LP states exist below the Fermi level in the sequence of Petrov *et al.*,⁷ while they appear both below and above the Fermi level in the sequence of Kooi and De Hosson.⁶ The splitting of Ge-Te bond reduces the population of LP electrons, which results in the partial occupation of the LP states. As the proximity of Ge layer to vacancy layer is responsible for the splitting, the electrical and optical properties should be more sensitive to the presence of Ge-Te-vacancy layers than Sb-Te-vacancy layers. Other partially occupied bands are derived from Sb-Te bonding, as observed in a theoretical study of the $\text{Ge}_1\text{Sb}_2\text{Te}_4$ phase.²⁰

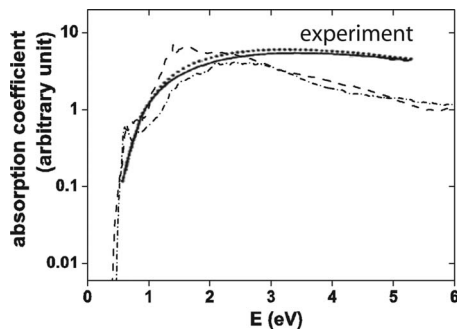


FIG. 4. Calculated absorption coefficients of hexagonal $\text{Ge}_2\text{Sb}_2\text{Te}_5$ with layer sequences of Kooi and De Hosson (Ref. 6) and Petrov *et al.* (Ref. 7). Dashed and dot-dashed lines correspond to the sequences of Kooi and De Hosson (Ref. 6) and Petrov *et al.* (Ref. 7), respectively. The solid and dotted lines represent the measurement for cubic and hexagonal phases, respectively (see Ref. 10). The layer sequence was not specified in the experiment.

The calculated band gaps are not consistent with measurement of the optical gap of about 0.5 eV for both the cubic and hexagonal phases.^{10,12} As the size of band gap is not well reproduced by the GGA, we calculate rather the absorption coefficient in order to see its dependence on the layer sequence. Figure 4 shows our calculated absorption coefficients for the hexagonal phase in both layer sequences. The

absorption edge is shifted for comparison to experiment.^{10,12} The cubic structure has almost the same absorption coefficients as the hexagonal phase for given layer sequences. Both layer sequences show a reasonable agreement with experiment, but the sequence of Petrov *et al.*⁷ seems to better fit the measurement.

In summary, we calculated the atomic and electronic structures and optical absorption coefficients of $\text{Ge}_2\text{Sb}_2\text{Te}_5$ by using the first principles method. It was found that the layer sequence has more profound effects than the crystal structure on these properties. For the sequence of Petrov *et al.*,⁷ the proximity of Ge to vacancy results in the splitting of Ge-Te bond, which reduces the Te lone-pair electrons that play a significant role in the electrical conduction. No splitting of Ge-Te bond is observed in the Kooi-De Hosson sequence. Calculated absorption coefficients show that the sequence of Petrov *et al.*⁷ better fits the measurement.

The authors appreciate the discussion with Jaymin Lee. This work was supported by the Korea Research Foundation Grant funded by the Korean government (MOEHRD, Basic Research Promotion Fund) (Grant No. KRF-2005-070-C00041). The authors would like to acknowledge the support from KISTI under the Ninth Strategic Supercomputing Support Program. G. L. was also partially supported by the SAIT.

*jhish@postech.ac.kr

¹M. Wuttig and N. Yamada, *Nat. Mater.* **6**, 824 (2007).

²A. V. Kolobov, P. Fons, A. I. Frenkel, A. L. Ankudinov, J. Tomimaga, and T. Uruga, *Nat. Mater.* **3**, 703 (2004).

³D. A. Baker, M. A. Paesler, G. Lucovsky, S. C. Agarwal, and P. C. Taylor, *Phys. Rev. Lett.* **96**, 255501 (2006).

⁴N. Yamada and T. Matsunaga, *J. Appl. Phys.* **88**, 7020 (2000).

⁵Y. J. Park, J. Y. Lee, M. S. Youm, Y. T. Kim, and H. S. Lee, *J. Appl. Phys.* **97**, 093506 (2005).

⁶B. J. Kooi and J. Th. M. De Hosson, *J. Appl. Phys.* **92**, 3584 (2002).

⁷I. I. Petrov, R. M. Imamov, and Z. G. Pinsker, *Sov. Phys. Crystallogr.* **13**, 339 (1968).

⁸T. Matsunaga, N. Yamada, and Y. Kabota, *Acta Crystallogr., Sect. B: Struct. Sci.* **60**, 685 (2004).

⁹Z. Sun, J. Zhou, and R. Ahuja, *Phys. Rev. Lett.* **96**, 055507 (2006).

¹⁰B.-S. Lee, J. R. Abelson, S. G. Bishop, D.-H. Kang, B. Cheong, and K.-B. Kim, *J. Appl. Phys.* **97**, 093509 (2005).

¹¹P. P. Konstantinov, L. E. Shelimova, E. S. Avilov, M. A. Kretova, and V. S. Zemskov, *Inorg. Mater.* **37**, 662 (2001).

¹²T. Kato and K. Tanaka, *Jpn. J. Appl. Phys.* **44**, 7340 (2005).

¹³A. Pirovano, A. L. Lacaita, A. Benvenuti, F. Pellizzer, and R. Bez, *IEEE Trans. Electron Devices* **51**, 452 (2004).

¹⁴G. Kresse and J. Hafner, *Phys. Rev. B* **47**, 558 (1993); G. Kresse and J. Furthmüller, *ibid.* **54**, 11169 (1996).

¹⁵J. P. Perdew and Y. Wang, *Phys. Rev. B* **45**, 13244 (1992).

¹⁶P. E. Blöchl, *Phys. Rev. B* **50**, 17953 (1994); G. Kresse and D. Joubert, *ibid.* **59**, 1758 (1999).

¹⁷V. Fiorentini, M. Methfessel, and M. Scheffler, *Phys. Rev. B* **47**, 13353 (1993).

¹⁸S.-H. Jhi and J. Ihm, *Phys. Status Solidi B* **191**, 387 (1995).

¹⁹S. Shamoto, N. Yamada, T. Matsunaga, Th. Proffen, J. W. Richardson, Jr., J.-H. Chung, and T. Egami, *Appl. Phys. Lett.* **86**, 081904 (2005).

²⁰W. Welnic, A. Pamungkas, R. Detemple, C. Steimer, S. Blugel, and M. Wuttig, *Nat. Mater.* **5**, 56 (2006).